

# Exploring entanglement in finite-size quantum systems with degenerate ground state

V.S. Okatev<sup>1</sup>, O.M. Sotnikov<sup>1</sup>, V.V. Mazurenko<sup>1</sup>

<sup>1</sup>*Theoretical Physics and Applied Mathematics Department,  
Ural Federal University, Mira Str. 19, 620002 Ekaterinburg, Russia*

We develop an approach for characterizing non-local quantum correlations in spin systems with exactly or nearly degenerate ground states. Starting with linearly independent degenerate eigenfunctions calculated with exact diagonalization we generate a finite set of their random linear combinations with Haar measure, which guarantees that these combinations are uniformly distributed in the space spanned by the initial eigenstates. Estimating the von Neumann entropy of the random wave functions helps to reveal previously unknown features of the quantum correlations in the phases with degeneracy of the ground state. For instance, spin spiral phase of the quantum magnet with Dzyaloshinskii-Moriya interaction is characterized by the enhancement of the entanglement entropy, which can be qualitatively explained by the changes in behaviour of two- and three-spin correlation functions. To establish the connection between our theoretical findings and real experiments we elaborate on the problem of estimating observables on the basis of the single-shot measurements of numerous degenerate eigenstates.

## INTRODUCTION

In quantum mechanics, if two or more different eigenfunctions of a Hamiltonian operator that describes a quantum system correspond to the same eigenenergy, they are degenerate and their arbitrary linear combination is likewise an eigenstate of the system. Degenerate quantum systems represent a special interest in condensed matter physics, theory of magnetism and quantum computing. For instance, the notable quantum Ising model characterized by two-fold degenerate ground state is widely used for benchmarking quantum algorithms<sup>1-3</sup> and platforms<sup>4,5</sup> as well as for demonstrating quantum priority<sup>6</sup>. Another important example is the Kitaev's toric code, degenerate quantum states employed in error correction algorithms<sup>7</sup>. From the side of fundamental research, the key role of degeneracy has been revealed when explaining the formation of a classical long-range order in a quantum system in the thermodynamic limit<sup>8-10</sup>.

Exploring the properties of the quantum systems with degenerate ground state is a hard numerical problem and is mainly performed with the family of the exact diagonalization methods having fundamental limitations on the size of the simulated systems<sup>11,12</sup>. Furthermore, some of the exact diagonalization approaches cannot resolve degeneracy correctly<sup>13,14</sup>. Employing neural quantum state approaches allows to work around the size limitation of the exact diagonalization and find the ground state energies of larger quantum systems. However, the accurate estimation of an observable in the case of a degenerate system generally represents a vast problem for neural-based approaches<sup>15</sup>. Linear combinations of the degenerate eigenstates obtained with exact diagonalization correspond to the same energy (Fig.1), but they can be of different complexity with respect to the amount of entanglement<sup>10</sup>, phase structure<sup>16,17</sup> and other quantum state properties<sup>18</sup>. This means that the theoretical description of a quantum system with degeneracy of the ground state is associated with the characterization of an ensemble of degenerate eigenfunctions that can be gen-

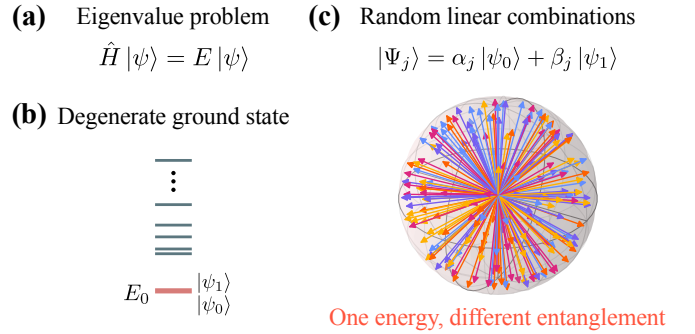


FIG. 1. The idea of our study. (a) We consider the eigenvalue problem for a given Hamiltonian with degenerate ground state that can be solved by means of exact diagonalization. (b) Schematic representation of an eigenspectrum of a system with two-fold degenerate ground state. (c) Random linear combinations of the degenerate eigenfunctions correspond to the same energy, but they can be characterized by different amount of the entanglement. Exploring quantum correlations of such a random eigenstates ensemble represents the main interest for us in this work.

erated on the basis of the exact diagonalization solutions (Fig.1). Surprisingly, to our knowledge, this problem has not yet been investigated.

From the experimental side, each preparation of the ground state of such a quantum system with adiabatic<sup>4</sup> or dissipative<sup>1</sup> protocols can result in a distinct wave function from degenerate eigensubspace. This should be taken into account when estimating different correlation functions on the basis of the projective measurements, which, in general, requires multiple copies of the same wave function.

In this paper we address the problem of characterizing degenerate ground states by the examples of the one-dimensional quantum Ising model and a two-dimensional spin system with Heisenberg and Dzyaloshinskii-Moriya interactions. Both models are characterized by the same mechanism of changing the degeneracy of the ground

state that is related to external magnetic field. First, to explore the ground state properties of these systems we generate finite sets of wave functions that belong to the degenerate eigensubspace and calculate the distributions of their von Neumann entropies. Remarkably, in the case of the model with non-collinear magnetic order, a previously unknown enhancement of the entanglement entropy of the degenerate states ensemble within the spin-spiral phase has been revealed. We show that such an enhancement correlates with change in behaviour of the spin-spin correlation functions at the same magnetic field values. Likewise, we consider the problem of reconstructing the simplest local spin correlation function by using the results of the projective measurements in the extreme case when before each measurement the system in question is prepared in a unrepeatable state from the degenerate manifold, which is relevant to the conditions of the real experiments.

## RESULTS

### A. Ising model

We start our investigation with analyzing the paradigmatic model in condensed matter physics that is transverse-field Ising Hamiltonian. Such a model for which the exact solution<sup>19</sup> is known since 1970 is still actively used for certifying various quantum algorithms<sup>2,3,18,20,21</sup>, testing utility of quantum computation with different platforms<sup>4-6</sup>, exploring non-equilibrium phases of matter<sup>22-24</sup> and solving other problems. The Ising Hamiltonian is given by

$$\hat{H}_{\text{Ising}} = \sum_{ij} J_{ij} \hat{S}_i^z \hat{S}_j^z + h \sum_i \hat{S}_i^x, \quad (1)$$

where  $\hat{S}_i^z$  and  $\hat{S}_i^x$  are the spin- $\frac{1}{2}$  operators,  $J_{ij}$  is the ferromagnetic exchange interaction between nearest neighbours along the chain and  $h$  is the  $x$ -oriented magnetic field. The considered system is characterized by the periodic boundary conditions. According to Ref.19 such a model features transition from ferromagnetic to paramagnetic states at the critical magnetic field value of  $0.5J$ .

Figure 2 gives the lowest energy part of the eigenspectrum of the 16-spin transverse-field Ising model obtained from exact diagonalization<sup>25</sup> with the nearest neighbour interaction  $J = -1$ . At the zero magnetic field the ground state of the Ising model is two-fold degenerate. Turning on the magnetic field leads to the opening of a gap between ground and first excited states, at the same time, the magnitude of the gap is of order of machine precision for weak fields as can be seen from Fig.2. Increasing the magnetic field gradually enlarges the energy gap and at the critical point one has  $\Delta = 0.0246$  which is an order of magnitude smaller than the splitting between first and second excited states at the same field. From the perspective of realizing the Ising model in real experiments at finite temperatures, for instance with Rydberg

atoms<sup>26</sup> and trapped ions<sup>27</sup>, the ground and first excited states of the Ising model within the ferromagnetic phase can be safely considered as being nearly degenerate.

Now we will turn to the analysis of the entanglement entropy that is of special interest in the case of the Ising model due to the possibility of analytical treatment<sup>28,29</sup>. The gist of the problem we are going to solve in this paper can be demonstrated by the example of the zero magnetic field Ising model for which the ground states of  $n$ -spin system are the trivial wave functions,  $|\varphi_1\rangle = |\uparrow\rangle^{\otimes n}$  and  $|\varphi_2\rangle = |\downarrow\rangle^{\otimes n}$ . Since each wave function is the tensor product of states of individual spins, they are non-entangled ones and the von Neumann entropy calculated for the reduced density matrix of a subsystem A,  $\mathcal{S}_{\text{vN}}(\rho_A) = -\text{Tr} \rho_A \log_2 \rho_A$  is zero. We would like to stress that one can choose a different set of wave functions  $|\varphi_+\rangle = \frac{1}{\sqrt{2}}(|\uparrow\rangle^{\otimes n} + |\downarrow\rangle^{\otimes n})$  and  $|\varphi_-\rangle = \frac{1}{\sqrt{2}}(|\uparrow\rangle^{\otimes n} - |\downarrow\rangle^{\otimes n})$  to define the two-fold degenerate ground state of the Ising model. In this case we deal with more complex wave functions whose entanglement entropy  $\mathcal{S}_{\text{vN}}(\rho_A) = 1$  for any subsystem A.

This simple example with different choices of the eigenstates clearly shows that entanglement properties of the degenerate ground states can be very diverse, as likewise found in the DMRG study of the Ising model<sup>30</sup>. From our point of view, a complete theoretical description of

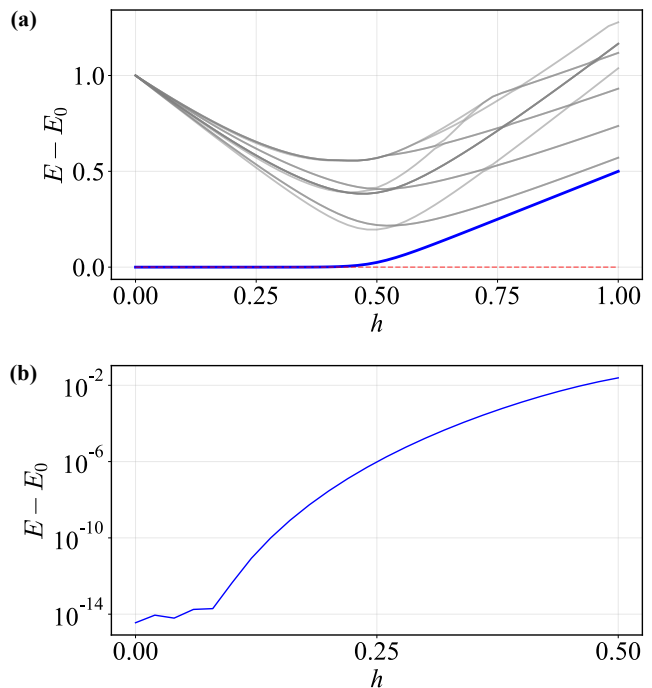


FIG. 2. (a) The calculated energies of the 16 low-lying eigenstates of the 16-spin Ising model in the transverse magnetic field, Eq.1. At each magnetic field the energies are shifted with respect to the ground state one (red dashed line). (b) Energy gap between ground and first excited states obtained for the ferromagnetic phase of the transverse-field Ising model. At  $h = 0.5$  the energy gap is equal to 0.0246.

the entanglement entropy of the degenerate eigenstates should be based on consideration of their ensemble and the main question is how to generate such an ensemble. Put another way, one is to specify the way of generating the complex random coefficients,  $\alpha_0, \alpha_2, \dots, \alpha_{\mathcal{D}-1}$  (where  $\mathcal{D}$  is the degeneracy degree) for linear combinations of the linearly independent degenerate wave functions,  $\{|\psi_d\rangle\}_{d=0..\mathcal{D}-1}$  obtained from exact diagonalization. Assuming that the resulting eigenstates should be uniformly distributed in the state space spanned with the wave functions  $\{|\psi_d\rangle\}_{d=0..\mathcal{D}-1}$ , the real and imaginary parts of the coefficients  $\{\alpha_d\}_{d=0..\mathcal{D}-1}$  are independently chosen from the normal distribution with zero mean<sup>31</sup> and, then, thus obtained vector is normalized. As we will show below such a procedure provides invariance of the ensemble properties to the choice of the initial eigenvectors,  $\{|\psi_d\rangle\}_{d=0..\mathcal{D}-1}$ . In this work the degeneracy degrees are  $\mathcal{D} = 2$  (Ising model) and  $\mathcal{D} = 6$  (DMI model), which defines the dimensions of the corresponding eigenvectors

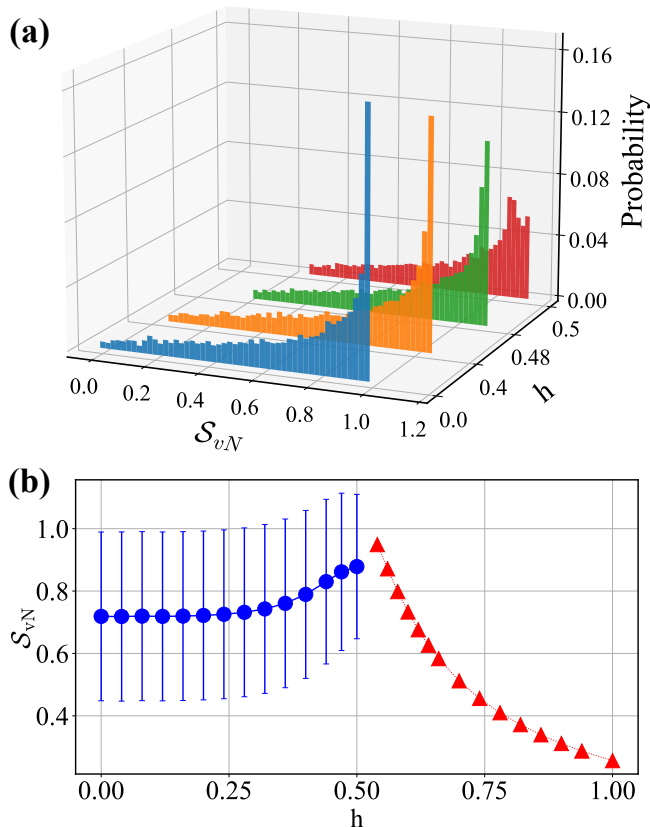


FIG. 3. (a) Distributions of the von Neumann entropy values calculated for 8192 samples at the different magnetic fields corresponding to the degenerate regime of the one-dimensional Ising model. (b) Dependence of the von Neumann entropy calculated for 16-qubit Ising model on the magnetic field. Error bar for the results obtained at  $h \in [0, 0.5]$  denotes the standard deviations of the entropies of the 8192 eigenstates generated by using Haar measure for degenerate ground states as described in the text.

subspaces.

Figure 3 (a) gives the entanglement distribution calculated for the following linear combinations of the degenerate eigenstates of the 16-spin Ising model

$$|\Psi\rangle = \alpha_0 |\psi_0\rangle + \alpha_1 |\psi_1\rangle. \quad (2)$$

Here  $|\psi_0\rangle$  and  $|\psi_1\rangle$  are the ground eigenstates taken from the exact diagonalization, and the random complex coefficients  $\alpha_0$  and  $\alpha_1$  are generated by using the Gaussian distribution as described above. Having generated 8192 different eigenstates  $|\Psi\rangle$  we have found that the probability of the samples with zero or small entanglement is close to zero. At the same time,  $\Pr(S_{vN})$  grows as the entanglement increases and achieves the maximal value at  $S_{vN}(\rho_A) = 1$ . As the result, the mean of the entanglement distribution is located at 0.75 and the corresponding standard deviation mainly covers the area of high entanglement (Fig. 3 (b)).

Numerical simulations of the ensembles each of which consists of 8192 eigenfunctions generated at finite magnetic fields with Eq.2 reveal the entanglement distributions similar to that for the zero-field case. For  $h < 0.25$  we observe a constant behaviour of the mean value of the calculated von Neumann entropy. Importantly, in the vicinity of the critical point  $h = 0.5$  there is an enhancement of the entanglement mean value. This agrees well with the results of the previous analytical considerations of the quantum correlations in the Ising model<sup>28,29</sup>. As we will show below other quantum systems with degenerate eigenstate can likewise feature enhancement of the entanglement. At  $h > 0.5$  the entanglement entropy has been calculated for non-degenerate ground states and demonstrates gradual decrease as the magnetic field increases. It approaches to zero in the limit of  $h \rightarrow \infty$ .

To demonstrate the importance of using the Gaussian distribution for sampling random coefficients in Eq.2 which corresponds to the Haar measure and provides the invariance of the ensemble properties with respect to the choice of the initial eigenstates, we consider two types of ground states superpositions:

$$\begin{aligned} |\Psi\rangle_d &= \alpha_0 |\uparrow\rangle^{\otimes n} + \alpha_1 |\downarrow\rangle^{\otimes n} \\ |\Psi\rangle_e &= \frac{\alpha_0}{\sqrt{2}} (|\uparrow\rangle^{\otimes n} + |\downarrow\rangle^{\otimes n}) + \frac{\alpha_1}{\sqrt{2}} (|\uparrow\rangle^{\otimes n} - |\downarrow\rangle^{\otimes n}) \end{aligned} \quad (3)$$

where  $\alpha_0$  and  $\alpha_1$  are random coefficients that can be generated with some distributions. The second equation can be rewritten as

$$|\Psi\rangle_e = \frac{\alpha_0 + \alpha_1}{\sqrt{2}} |\uparrow\rangle^{\otimes n} + \frac{\alpha_0 - \alpha_1}{\sqrt{2}} |\downarrow\rangle^{\otimes n}. \quad (4)$$

Then, one can express the von Neumann entropy for these superpositions as

$$\begin{aligned} \mathcal{S}_{vN}^d(\rho_A) &= -|\alpha_0|^2 \log_2 |\alpha_0|^2 - |\alpha_1|^2 \log_2 |\alpha_1|^2, \\ \mathcal{S}_{vN}^e(\rho_A) &= -\frac{|\alpha_0 + \alpha_1|^2}{2} \log_2 \frac{|\alpha_0 + \alpha_1|^2}{2} \\ &\quad - \frac{|\alpha_0 - \alpha_1|^2}{2} \log_2 \frac{|\alpha_0 - \alpha_1|^2}{2}, \end{aligned} \quad (5)$$

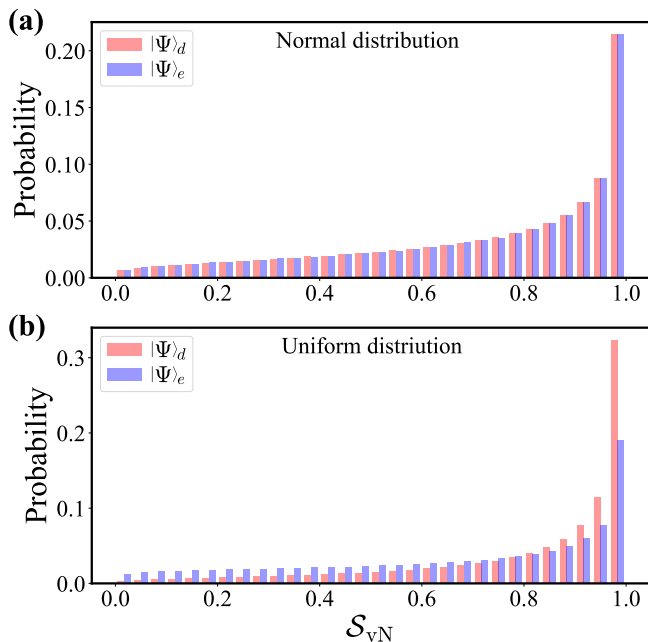


FIG. 4. Entropy distributions calculated for the superpositions of the entangled  $|\Psi_e\rangle$  and non-entangled  $|\Psi_d\rangle$  ground states of the zero-field Ising model. Data were obtained with (a) normal (Haar) and (b) uniform distributions for the linear combination coefficients.

where  $\rho_A$  is the reduced density matrix describing the subsystem A. With the expressions, Eq.5 it is possible to sample entropy of arbitrary size system for different distribution laws of  $\alpha_0$  and  $\alpha_1$  random variables.

Figure 4 demonstrates the examples of the entropy distributions for  $|\Psi_d\rangle$  and  $|\Psi_e\rangle$  states when the real and imaginary parts of the coefficients are generated by using either uniform distribution in range  $(-1,1)$  or Gaussian distribution with zero mean and unit variance. While for the Gaussian case we observe invariance of the resulting entanglement distribution with respect to the initial states used for ensemble creation (Fig. 4 (a)), it is not the case for the results obtained with the uniform distribution (Fig. 4 (b)).

### B. Quantum model with non-collinear magnetic ordering

As a more complicated example of the quantum system with degeneracy of the ground state we consider the Heisenberg Hamiltonian with Dzyaloshinskii-Moriya interaction defined on a 19-site triangular supercell with periodic boundary conditions:

$$\hat{H}_{\text{DMI}} = \sum_{i>j} J_{ij} \hat{\mathbf{S}}_i \cdot \hat{\mathbf{S}}_j + \sum_{i>j} \mathbf{D}_{ij} \cdot [\hat{\mathbf{S}}_i \times \hat{\mathbf{S}}_j] + h \sum_i \hat{S}_i^z \quad (6)$$

where  $J_{ij}$  and  $\mathbf{D}_{ij}$  are isotropic and Dzyaloshinskii-Moriya interactions. In the previous works<sup>10,32</sup> it has

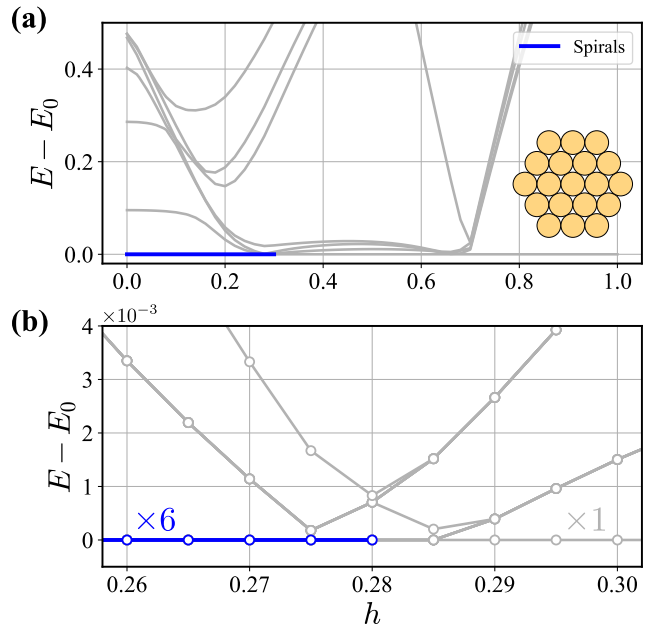


FIG. 5. (a) Magnetic-field dependence of the low-energy part of the eigenspectrum calculated for the Heisenberg model with Dzyaloshinskii-Moriya interaction, Eq.6. The model is defined on the 19-spin plaquette (inset). (b) Zoom view of the transitional area between the spin-spiral and skyrmion phases. Blue line denotes 6-fold degenerate spin-spiral ground state.

been shown that depending on the value of the magnetic field such a model taken with the ferromagnetic exchange  $J = -0.5$  and in-plane Dzyaloshinskii-Moriya interactions  $|\mathbf{D}_{ij}| = 1$  can be in either collinear ferromagnetic or non-collinear, quantum spin spiral or quantum skyrmion states. The origin of these quantum phases has been established by analyzing the calculated magnetization, spin structural factors, scalar chirality as well as by comparing quantum and classical solutions. Here we primarily focus on a still poorly understood issue, which concerns the entanglement properties of the spin spiral phase characterized by degeneracy of ground eigenstates.

According to the eigenspectra obtained from exact diagonalization and presented in Fig. 5 there is the sixfold degenerate ground state ( $0 \leq h \leq 0.28$ ) that is denoted with blue, associated to spin spiral state and represents the main interest for us in this work. In turn, the degeneracy is lifted for  $h \in (0.28, 0.66)$ . Then, there is a very narrow range  $[0.66, 0.68]$  that is characterized by the six-fold degenerate ground state. For  $h > 0.68$  the ground state is non-degenerate. Taking into account the behaviour of the excited states one can distinguish two different regimes for  $0.28 < h < 0.68$  and  $h > 0.68$ . For the former 18 excited states having the energies that are close to the ground state are well separated from the rest and, thus they can be considered to be a part of nearly 19-fold degenerate ground state. This point was discussed in details in Ref.<sup>10</sup>. In turn, the high field region is de-



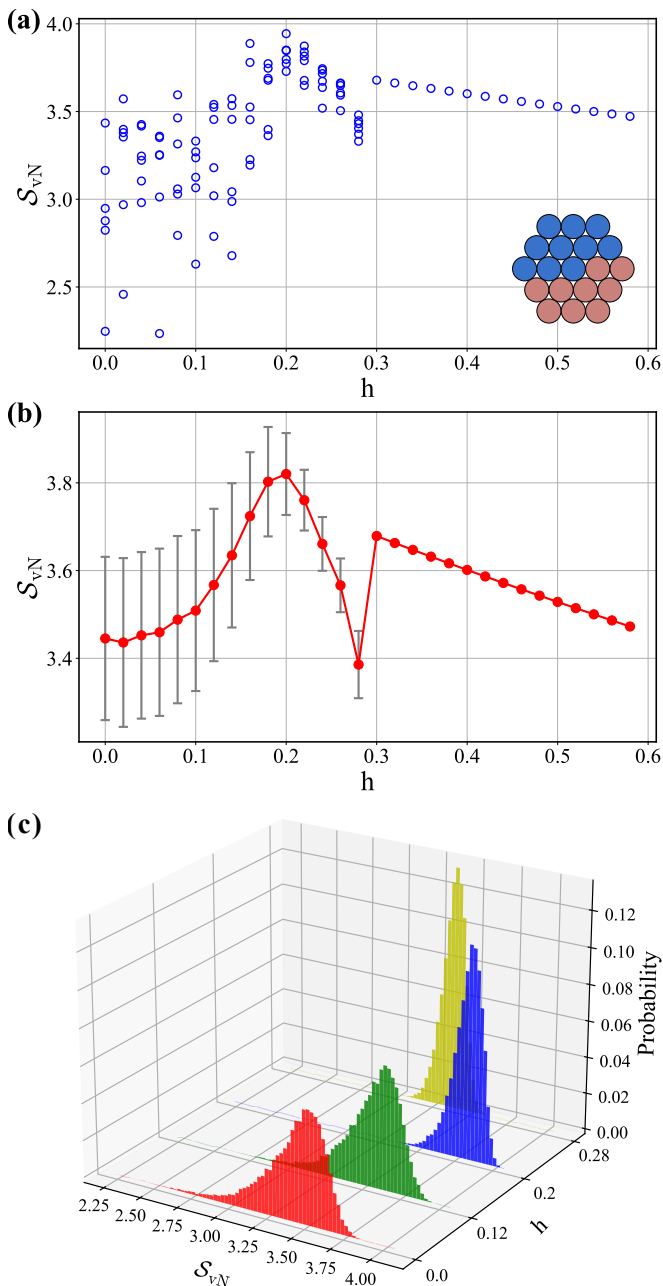


FIG. 6. (a) Entanglement entropy of the eigenfunctions obtained by using the exact diagonalization of the DMI-model, Eq.6 at different magnetic fields. The inset shows the used bipartition of the system in question. (b) Mean and standard deviation of the entanglement entropy calculated for 22528 random eigenvectors superpositions generated with Haar measure in the range  $h \in [0, 0.28]$  as described in the text. (c) Distributions of the calculated entanglement entropy within the spin spiral phase.

scribed by the pure ferromagnetic ground state that is well-separated from excited levels.

We are now in a position to perform a preliminary analysis of the quantum correlations of the system being in the spin spiral phase with degenerate ground state for

$0 \leq h \leq 0.28$ . Fig. 6 (a) shows entanglement entropies for six eigenstates obtained from exact diagonalization of the spin model, Eq.6 at different magnetic fields. Fluctuations of the entropy values are significant and random. We do not observe any pattern in  $\mathcal{S}_{vN}$ . Similar picture of data fluctuations when one calculating the topological entropy for a related model with degeneracy of the ground state was previously reported in Ref.33. The entropy variance becomes smaller for  $h$  close to 0.2.

Following the entanglement analysis of the Ising model presented above in the case of the DMI Hamiltonian we have generated 22528 samples of the degenerate eigenstates from six initial ones,  $|\psi_d\rangle$  ( $d = 0, \dots, 5$ ) obtained from the exact diagonalization. In order to make thus generated eigenfunctions,  $|\Psi\rangle = \sum_d \alpha_d |\psi_d\rangle$  uniformly distributed over the six-dimensional subspace spanned by  $|\psi_d\rangle$  vectors, the random complex coefficients are chosen according to the normal distribution. Figures 6 (b) and (c) demonstrate the entanglement behaviour of the degenerate ground states ensemble. The profile of the entanglement distribution (Fig. 6 (c)) is close to Gaussian one and differs from the Ising model result. The entropy averaged over the ensemble features the maximum at  $h = 0.2$  and function discontinuity in the vicinity of  $h = 0.28$ .

The behaviour of the von Neumann entropy  $\mathcal{S}_{vN}(\rho_A)$  for  $h \in (0.28, 0.3)$  can be attributed to the transition from quantum spin spiral to quantum skyrmion states and observed in the previous studies<sup>34</sup>. To confirm the existence of the quantum skyrmion state in Fig.7 we reproduce the average zero-temperature value of the scalar chirality operator introduced in Ref.<sup>32</sup>

$$Q_\Psi = \frac{N_\Delta}{\pi} \langle \hat{\mathbf{S}}_1 [\hat{\mathbf{S}}_2 \times \hat{\mathbf{S}}_3] \rangle, \quad (7)$$

where  $N_\Delta$  is the number of non-overlapping triangles between nearest neighbours. The correlator in this equation is defined as  $\langle \hat{X} \rangle = \frac{1}{\mathcal{D}} \sum_d \langle \psi_d | \hat{X} | \psi_d \rangle$ , where  $\mathcal{D}$  is the degeneracy degree of the ground state and  $|\psi_d\rangle$  is the eigenstate obtained with the exact diagonalization. The calculated  $Q_\Psi$  is characterized by the plateau in the range  $0.3 \leq h < 0.68$ , which is the signature of forming pure quantum skyrmion state.

According to the results of previous investigations<sup>32</sup> at  $h = 0$  the system in question is found to be in the pure spin-spiral state. There are six Bragg peaks at opposite wave vectors  $\mathbf{q}$  and  $-\mathbf{q}$  and zero chirality. In turn, in the range of the fields  $0 < h < 0.28$  the system reveals properties inherent both quantum spin spiral and skyrmion phases. Interestingly, the peak of the entanglement entropy at  $h = 0.2$  (Fig. 6 (b)) evidences some changes in quantum correlations, which have not discussed in the previous works.

To elaborate this point we have analyzed Ursell spin-spin correlation functions<sup>35</sup>

$$\Gamma_{ij}^{zz} = \langle S_i^z S_j^z \rangle - \langle S_i^z \rangle \langle S_j^z \rangle \quad (8)$$

between nearest and next-nearest neighbours as well as

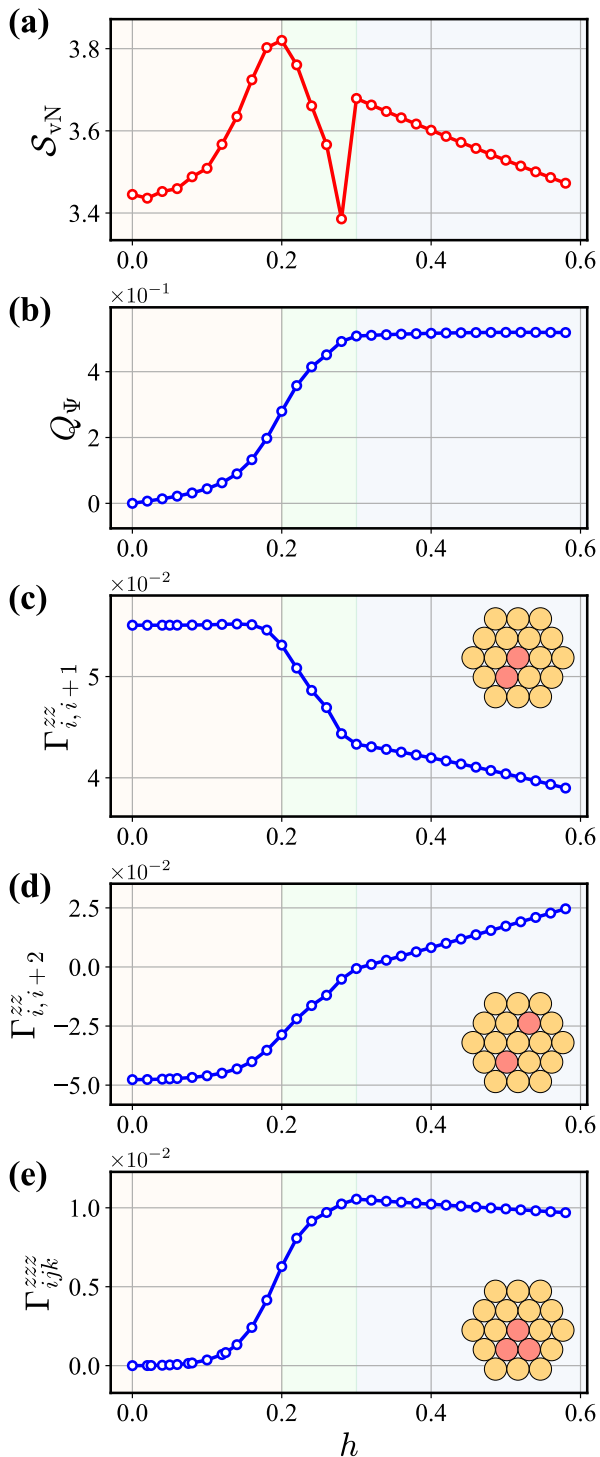


FIG. 7. (a) Mean values of the entanglement entropy reproduced from Fig.6 (b). (b) Scalar chirality calculated with Eq.7. (c) and (d) Two-spin Ursell functions, Eq.8 estimated for nearest and next-nearest neighbour spins, respectively. (e) Three-spin Ursell function calculated with Eq.9. Background colors denote spin-spiral (yellow), intermediate (green) and (blue) skyrmionic (blue) phases.

three-spin  $zzz$  correlation function for an arbitrary triangle of neighbouring spins

$$\Gamma_{ijk}^{zzz} = \langle S_i^z S_j^z S_k^z \rangle - 3 \langle S_i^z \rangle \langle S_j^z S_k^z \rangle + 2 \langle S_i^z \rangle \langle S_j^z \rangle \langle S_k^z \rangle. \quad (9)$$

The results of these calculations presented in Fig.7 show constant ferromagnetic behaviour of the pair correlation function for the nearest neighbour spins in the range of the fields  $0 < h < 0.2$ . For the fields higher than 0.2 we observe a suppression of  $\Gamma_{ij}^{zz}$ . As for the next-nearest neighbours correlations, they are antiferromagnetic, demonstrate constant behaviour at  $0 \leq h < 0.15$  and are suppressed at higher magnetic fields. Interestingly, at the critical fields  $h \in (0.28, 0.3)$  corresponding to the transition from the spin spiral to the skyrmion phase, the  $\Gamma_{ij}^{zz}$  correlator for next-nearest neighbours is zero. Contrary to the pair Ursell functions, three-spin correlations ( $\Gamma_{ijk}^{zzz}$ ) demonstrates the opposite trend, they amplify with increasing the magnetic field, which is similar to the behaviour of the scalar chirality discussed above.

### C. Single-shot description of the degenerate systems

Having quantified quantum correlations of the ensembles of the degenerate eigenstates for two correlated systems with von Neumann entropy we are going to consider the characterization of the same quantum systems on the level of the projective measurements. Normally, in quantum computing or atomic simulations one prepares multiple copies of a given quantum state and performs their projective measurements<sup>36</sup>. It allows to estimate correlation functions<sup>37,38</sup>, entanglement entropy<sup>2,7,37</sup> or other measures<sup>18,39-42</sup> for describing the system in question. In the degenerate case we consider multiple copies of the same eigenstate may not be available in real experiments<sup>1,4</sup>. That is why it is instructive to imitate an extreme situation when every eigenstate that is prepared for measurement belongs to the degenerate manifold and is measured only once. A finite set of the bitstrings obtained within such a single-shot protocol contains some information on the degenerate manifold of the ground state. However, the usefulness of these data is not a priori obvious and requires additional study.

In our work we focus on estimating the local correlation function in the ground state that can be formally written as

$$\langle \hat{S}_i^\mu \rangle = \frac{1}{\mathcal{D}} \sum_d \langle \psi_d | \hat{S}_i^\mu | \psi_d \rangle, \quad (10)$$

where the index  $d$  denotes degenerate eigenstates,  $\mu$  stands for projection of the spin operator and  $i$  is the site index. For the models we consider the local magnetization can be calculated exactly. In Fig.8 we present these exact values of the local magnetization with lines. Blue color denotes the range of the magnetic fields with degenerate solutions. These results fully agree with that known from the literature<sup>19</sup>.

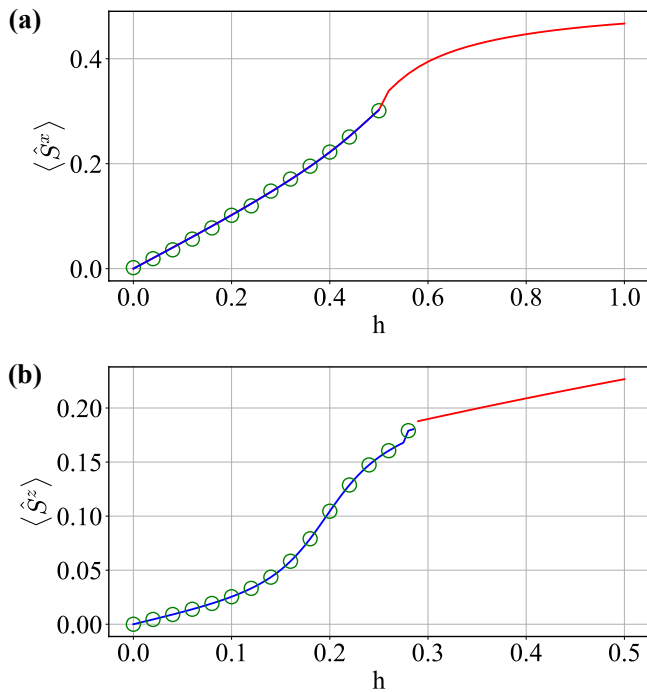


FIG. 8. Calculated magnetizations and the corresponding approximations obtained within single-shot protocol for (a) Ising model and (b) DMI Hamiltonian. Red lines denote the magnetization for non-degenerate ground state taken from exact diagonalization. Blue lines stand for results obtained with 2-fold (Ising model) and 6-fold (DMI model) degenerate eigenfunctions. Circles correspond to the magnetization values, Eq.11 averaged over ensemble of the degenerate eigenstates by using single-shot protocol described in the text.

We are now in a position to define an analog of the local correlation function that can be estimated from the single-shot protocol for degenerate eigenstates described above. More specifically, for each site we are to estimate the following quantity

$$\langle \hat{S}^\mu \rangle_{\text{Haar}} = \frac{p(\uparrow) - p(\downarrow)}{2}, \quad (11)$$

where  $p(\uparrow)$  ( $p(\downarrow)$ ) is the probability to get the spin-up (spin-down) state for the given site when performing measurements. This quantity is estimated for a finite set of the degenerate eigenstates superpositions generated with the normal distribution law. Practically, the probability function is estimated from the finite set of bit-

strings obtained with single-shot protocol. The number of the bitstrings is equal to 8192 and 256 for the Ising and DMI models, respectively. The basis for measurements is defined by the direction of the external magnetic field in the considered model ( $x$  for Ising Hamiltonian and  $z$  for the DMI model). The calculated values of  $\langle \hat{S}^\mu \rangle_{\text{Haar}}$  averaged over spins are presented in Fig.8 with circles. One can see that the single-shot protocol provides reliable approximation of the exact data and can be used in real experiments dealing with degenerate quantum systems.

## CONCLUSION

In this work we address the problem of characterizing the quantum systems in degenerate ground states with a special focus on entanglement entropy properties. On the basis of the linearly independent degenerate eigenstates calculated with exact diagonalization we propose to generate a finite ensemble of their linear combinations with Haar measure. This allows to probe the entanglement distributions of the ground wave functions. The primers we consider in this work show that such distributions are problem specific. For instance, in the case of the transverse-field Ising model the calculated values of the von Neumann entropy are non-uniformly distributed in the wide range between 0 and 1. At the same time, for the quantum system with non-collinear order the entanglement distribution reveals a more localized Gaussian-like shape. The found enhancement of the mean entropy of the degenerate eigenstate ensemble in the spin spiral phase can be explained by the changes in three- and two-spin correlations which demonstrate different trends at increasing the external magnetic field. To establish a connection between our theoretical results and real experiments we analyze the important details concerning estimation of the observables in the case of the degenerate quantum systems.

## ACKNOWLEDGEMENTS

The research funding from the Ministry of Science and Higher Education of the Russian Federation (Ural Federal University Program of Development within the Priority-2030 Program, project 4.72) is gratefully acknowledged. Quantum simulations were performed on the Uran supercomputer at the IMM UB RAS.

<sup>1</sup> X. Mi et al., Stable quantum-correlated many-body states through engineered dissipation, *Science* 383, 1332–1337 (2024).

<sup>2</sup> Jun Yong Khoo and Markus Heyl, Quantum entanglement recognition, *Phys. Rev. Research* 3, 033135 (2021)

<sup>3</sup> G. Carleo and M. Troyer, M. Solving the quantum many-body problem with artificial neural networks. *Science* 355, 602–606 (2017).

<sup>4</sup> Pascal Scholl, Michael Schuler, Hannah J. Williams, Alexander A. Eberharter, Daniel Barredo, Kai-Niklas

- Schymik, Vincent Lienhard, Louis-Paul Henry, Thomas C. Lang, Thierry Lahaye, Andreas M. Läuchli and Antoine Browaeys, Quantum simulation of 2D antiferromagnets with hundreds of Rydberg atoms, *Nature* 595, 233 (2021)
- <sup>5</sup> P. Schauss, J. Zeiher, T. Fukuhara, S. Hild, M. Cheneau, T. Macri, T. Pohl, I. Bloch, C. Gross, Crystallization in Ising quantum magnets, *Science* 347, 1455 (2015).
  - <sup>6</sup> Youngseok Kim, Andrew Eddins, Sajant Anand, Ken Xuan Wei, Ewout van den Berg, Sami Rosenblatt, Hasan Nayfeh, Yantao Wu, Michael Zaletel, Kristan Temme and Abhinav Kandala, Evidence for the utility of quantum computing before fault tolerance, *Nature* 618, 500 (2023).
  - <sup>7</sup> K. J. Satzinger, Y. Liu, A. Smith, C. Knapp, M. Newman, C. Jones, Z. Chen, C. Quintana, X. Mi, A. Dunsworth, C. Gidney, I. Aleiner, F. Arute, K. Arya, J. Atalaya, R. Babush, J. C. Bardin, R. Barends, J. Basso, A. Bengtsson, A. Bilmes, M. Broughton, B. B. Buckley, D. A. Buell, B. Burkett, N. Bushnell, B. Chiaro, R. Collins, W. Courtney, S. Demura, A. R. Derk, D. Eppens, C. Erickson, E. Farhi, L. Foaro, A. G. Fowler, B. Foxen, M. Giustina, A. Greene, J. A. Gross, M. P. Harrigan, S. D. Harrington, J. Hilton, S. Hong, T. Huang, W. J. Huggins, L. B. Ioffe, S. V. Isakov, E. Jeffrey, Z. Jiang, D. Kafri, K. Kechedzhi, T. Khattar, S. Kim, P. V. Klimov, A.N. Korotkov, F. Kostritsa, D. Landhuis, P. Laptev, A. Locharla, E. Lucero, O. Martin, J. R. McClean, M. McEwen, K. C. Miao, M. Mohseni, S. Montazeri, W. Mroczkiewicz, J. Mutus, O. Naaman, M. Neeley, C. Neill, M. Y. Niu, T. E. O'Brien, A. Opremcak, B. Pató, A. Petukhov, N. C. Rubin, D. Sank, V. Shvarts, D. Strain, M. Szalay, B. Villalonga, T. C. White, Z. Yao, P. Yeh, J. Yoo, A. Zalcman, H. Neven, S. Boixo, A. Megrant, Y. Chen, J. Kelly, V. Smelyanskiy, A. Kitaev, M. Knap, F. Pollmann, P. Roushan, Realizing topologically ordered states on a quantum processor, *Science* 374, 1237-1241 (2021).
  - <sup>8</sup> P. W. Anderson, An approximate quantum theory of the antiferromagnetic ground state, *Phys. Rev.* 86, 694 (1952).
  - <sup>9</sup> A. Wietek, M. Schuler, and A.M. Läuchli, Studying continuous symmetry breaking using energy level spectroscopy, arXiv:1704.08622.
  - <sup>10</sup> O.M. Sotnikov, E.A. Stepanov, M.I. Katsnelson, F. Mila, V.V. Mazurenko, Emergence of Classical Magnetic Order from Anderson Towers: Quantum Darwinism in Action, *Physical Review X* 13, 041027 (2023).
  - <sup>11</sup> A. M. Läuchli, J. Sudan, and E. S. Sørensen, Ground-state energy and spin gap of spin-1 kagome-Heisenberg antiferromagnetic clusters: Large-scale exact diagonalization results, *Phys. Rev. B* 83, 212401 (2011)
  - <sup>12</sup> A. Wietek and A. M. Läuchli, Sublattice coding algorithm and distributed memory parallelization for large-scale exact diagonalizations of quantum many-body systems, *Phys. Rev. E* 98, 033309 (2018)
  - <sup>13</sup> Alexander Weisse and Holger Fehske, Exact Diagonalization Techniques, *Lecture Notes in Physics* 739, 529 (2008).
  - <sup>14</sup> R.M. Noack and S. Manmana, Diagonalization- and Numerical Renormalization-Group-Based Methods for Interacting Quantum Systems, *AIP Conf. Proc.* 789, 93 (2005)
  - <sup>15</sup> Ashish Joshi, Robert Peters, and Thore Posske, Ground state properties of quantum skyrmions described by neural network quantum states, *Phys. Rev. B* 108, 094410 (2023).
  - <sup>16</sup> T. Westerhout, N. Astrakhantsev, K. S. Tikhonov, M. I. Katsnelson, and A. A. Bagrov, Generalization properties of neural network approximations to frustrated magnet ground states, *Nat. Commun.* 11, 1593 (2020)
  - <sup>17</sup> Tom Westerhout, Mikhail I. Katsnelson, Andrey A. Bagrov, Many-body quantum sign structures as non-glassy Ising models, *Communications Physics* 6, 275 (2023).
  - <sup>18</sup> O.M. Sotnikov, I.A. Iakovlev, A. A. Iliasov, M. I. Katsnelson, A. A. Bagrov, V.V. Mazurenko, Certification of quantum states with hidden structure of their bitstrings, *npj Quantum Information* 8, 41 (2022).
  - <sup>19</sup> P. Pfeuty, The one-dimensional Ising model with a transverse field, *Ann. Phys. (N.Y.)* 57, 79 (1970)
  - <sup>20</sup> P. Q. Cruz, G. Catarina, R. Gautier, J. Fernández-Rossier, Optimizing quantum phase estimation for the simulation of Hamiltonian eigenstates, *Quantum Sci. Technol.* 5 044005 (2020).
  - <sup>21</sup> Wen Wei Ho, Timothy H. Hsieh, Efficient variational simulation of non-trivial quantum states, *SciPost Phys.* 6, 029 (2019).
  - <sup>22</sup> Matteo Ippoliti, Kostyantyn Kechedzhi, Roderich Moessner, S.L. Sondhi, and Vedika Khemani, Many-Body Physics in the NISQ Era: Quantum Programming a Discrete Time Crystal, *PRX QUANTUM* 2, 030346 (2021)
  - <sup>23</sup> X. Mi et al., Time-crystalline eigenstate order on a quantum processor, *Nature (London)* 601, 531 (2022).
  - <sup>24</sup> E. A. Maletskii, I. A. Iakovlev, and V. V. Mazurenko, Quantifying spatiotemporal patterns in classical and quantum systems out of equilibrium, *Phys. Rev. E* 109, 024105 (2024)
  - <sup>25</sup> T. Westerhout, Lattice-symmetries: A package for working with quantum many-body bases, *J. Open Source Software* 6, 3537 (2021).
  - <sup>26</sup> H. Bernien, S. Schwartz, A. Keesling, H. Levine, A. Omran, H. Pichler, S. Choi, A.S. Zibrov, M. Endres, M. Greiner, V. Vuletić and M.D. Lukin, Probing many-body dynamics on a 51-atom quantum simulator, *Nature* 551(7682), 579 (2017).
  - <sup>27</sup> C. Monroe, W.C. Campbell, L.-M. Duan, Z.-X. Gong, A.V. Gorshkov, P.W. Hess, R. Islam, K. Kim, N.M. Linke, G. Pagano, P. Richerme, C. Senko, and N.Y. Yao, Programmable quantum simulations of spin systems with trapped ions, *Rev. Mod. Phys.* 93, 025001 (2021).
  - <sup>28</sup> J. I. Latorre, E. Rico and G. Vidal, Ground state entanglement in quantum spin chains, *Quantum Inf. Comput.* 4, 048 (2004)
  - <sup>29</sup> P. Calabrese and J. Cardy, Entanglement entropy and quantum field theory, *Journal of Statistical Mechanics: Theory and Experiment* 2004(06), P06002 (2004)
  - <sup>30</sup> I. Peschel, M. Kaulke, Ö. Legeza, Density-matrix spectra for integrable models, *Ann. Physik (Leipzig)* 8, 153 (1999).
  - <sup>31</sup> Karol Zyczkowski and Hans-Jürgen Sommers, Induced measures in the space of mixed quantum states, *Journal of Physics A: Mathematical and General* 34, 7111 (2001).
  - <sup>32</sup> O.M. Sotnikov, V.V. Mazurenko, J. Colbois, F. Mila, M.I. Katsnelson, and E.A. Stepanov, Probing the topology of the quantum analog of a classical skyrmion, *Phys. Rev. B* **103**, L060404 (2021)
  - <sup>33</sup> Vipin Vijayan, L. Chotorlishvili, A. Ernst, S. S. P. Parkin, M. I. Katsnelson, S. K. Mishra, Topological entanglement entropy to identify topological order in quantum skyrmions, arXiv:2311.03915.
  - <sup>34</sup> Andreas Haller, Solofo Groenendijk, Alireza Habibi, Andreas Michels, and Thomas L. Schmidt, Quantum skyrmion lattices in Heisenberg ferromagnets, *Phys. Rev. Research* 4, 043113 (2022).



- <sup>35</sup> H.D. Ursell, The evaluation of Gibbs' phase-integral for imperfect gases, in *Mathematical Proceedings of the Cambridge Philosophical Society*, Vol. 23 (Cambridge University Press, 1927) pp. 685–697.
- <sup>36</sup> Michael A. Nielsen and Isaac L. Chuang, *Quantum Computation and Quantum Information* (Cambridge University Press, 2000)
- <sup>37</sup> H.-Y. Huang, R. Kueng, and J. Preskill, Predicting many properties of a quantum system from very few measurements. *Nat. Phys.* 16, 1050–1057 (2020).
- <sup>38</sup> Oleg M. Sotnikov, Ilia A. Iakovlev, Evgeniy O. Kiktenko, Mikhail I. Katsnelson, Aleksey K. Fedorov, Vladimir V. Mazurenko, Emergence of global receptive fields capturing multipartite quantum correlations, arXiv: 2408.13033.
- <sup>39</sup> Oleg M. Sotnikov, Ilia A. Iakovlev, Evgeniy O. Kiktenko, Aleksey K. Fedorov, Vladimir V. Mazurenko, Achieving the volume-law entropy regime with random-sign Dicke states, arXiv:2404.15050
- <sup>40</sup> Vladimir V Mazurenko, Ilia A Iakovlev, Oleg M Sotnikov, Mikhail I Katsnelson, Estimating patterns of classical and quantum skyrmion states, *Journal of the Physical Society of Japan* 92, 081004 (2023).
- <sup>41</sup> Ilia A. Iakovlev, Oleg M. Sotnikov, Ivan V. Dyakonov, Evgeniy O. Kiktenko, Aleksey K. Fedorov, Stanislav S. Straupe, Vladimir V. Mazurenko, Benchmarking a boson sampler with Hamming nets, *Phys. Rev. A* 108, 062420 (2023).
- <sup>42</sup> O.M. Sotnikov and V.V. Mazurenko, Neural network agent playing spin Hamiltonian games on a quantum computer, *J. Phys. A: Math. Theor.* 53 135303 (2020).